

Learning Evolution via Optimization Knowledge Adaptation

Chao Wang¹, Licheng Jiao^{1*}, Jiaxuan Zhao¹, Lingling Li¹,
Fang Liu¹, Shuyuan Yang¹

^{1*}School of Artificial Intelligence, Xidian University, No. 2 South Taibai Road, Xi'an, 710071, Shaanxi, China.

*Corresponding author(s). E-mail(s): lchjiao@mail.xidian.edu.cn;
Contributing authors: xiaofengxd@126.com;
jiaxuanzhao@stu.xidian.edu.cn; lli@xidian.edu.cn; f63liu@163.com;
syyang@xidian.edu.cn;

Abstract

Evolutionary algorithms (EAs) maintain populations through evolutionary operators to discover diverse solutions for complex tasks while gathering valuable knowledge, such as historical population data and fitness evaluations. However, traditional EAs face challenges in dynamically adapting to expanding knowledge bases, hindering the efficient exploitation of accumulated information and limiting adaptability to new situations. To address these issues, we introduce an Optimization Knowledge Adaptation Evolutionary Model (OKAEM), which features dynamic parameter adjustment using accumulated knowledge to enhance its optimization capabilities. OKAEM employs attention mechanisms to model the interactions among individuals, fitness landscapes, and genetic components separately, thereby parameterizing the evolutionary operators of selection, crossover, and mutation. These powerful learnable operators enable OKAEM to benefit from pre-learned extensive prior knowledge and self-tune with real-time evolutionary insights. Experimental results demonstrate that OKAEM: 1) exploits prior knowledge for significant performance gains across various knowledge transfer settings; 2) achieves competitive performance through self-tuning alone, even without prior knowledge; 3) outperforms state-of-the-art black-box baselines in a vision-language model tuning case; 4) can improve its optimization capabilities with growing knowledge; 5) is capable of emulating principles of natural selection and genetic recombination.

Keywords: Neural and Evolutionary Computing, Knowledge Transfer, Adaptation

1 Introduction

Inspired by biological evolution, evolutionary algorithms (EAs) continuously update population systems through crossover, mutation, and selection to explore complex fitness landscapes [1]. Prominent examples of EAs include the genetic algorithm (GA) [2], the evolution strategy (ES) [3], and the genetic programming (GP) [4]. These methods rely solely on the fitness values of individuals to drive the evolutionary process without requiring gradient information. Advances in computational techniques [5] have allowed EAs to provide diverse solutions for highly complex optimization tasks such as neuroevolution [6, 7], robotic control [8, 9], industrial design [10], and scientific discoveries [11, 12]. As the scale and complexity of these tasks increase [1, 13], EAs generate a significant amount of valuable knowledge, including historical populations and their fitness data. However, existing EAs face challenges in enhancing their optimization capabilities as knowledge bases grow. Two long-standing issues are particularly prominent: incomplete utilization of prior knowledge and inflexible knowledge adaptation strategies.

Evolutionary knowledge transfer (EKT) leverages prior knowledge from source tasks to accelerate evolutionary optimization for challenging target tasks [14–20]. Current mainstream EKT methods focus mainly on knowledge derived from highly related individuals [21], thus neglecting valuable information from other candidates within the population. This limited knowledge utilization hampers the exploitation of underlying evolutionary behaviors on source tasks. Furthermore, adaptability has long been a key challenge in the field of EAs [2, 22–24]. The absence of a unified framework for heuristic evolutionary operators results in adaptability strategies specific to particular EAs. For example, the covariance matrix adaptation used in evolution strategies (CMAES) [25] may not be effective in GA contexts. Recent studies [26–30] have explored training parameterized EAs in various tasks to improve generalization and adaptability. However, these learnable EAs (LEAs) cannot dynamically adjust parameters using generated populations and fitness data, potentially limiting their optimization capabilities.

To address these challenges, we introduce the Optimization Knowledge Adaptation Evolutionary Model (OKAEM), which exhibits powerful transferability and adaptability. OKAEM pre-learns extensive prior knowledge from source tasks and dynamically adjusts to incorporate new knowledge from target tasks. By leveraging attention mechanisms, OKAEM explicitly models the relationships among individuals, fitness landscapes, and genetic components, guiding selection, crossover, and mutation. These parameterized evolutionary operators enable learnable and highly parallelizable update rules. Multilayer perceptrons (MLPs) with Dropout are employed to introduce stochasticity into the operators. To our knowledge, this is the first instance where neurons are used to represent the random behavior in EAs.

OKAEM involves two stages: pre-training and adaptive optimization (Fig. 1). During the pre-training stage, OKAEM learns population evolution behaviors on source tasks by predicting the next generation’s population, thereby leveraging prior knowledge to enhance performance. In the adaptive optimization phase, OKAEM continuously generates offspring and dynamically tunes its parameters to adapt to new evolutionary insights by minimizing the distance between generated populations and

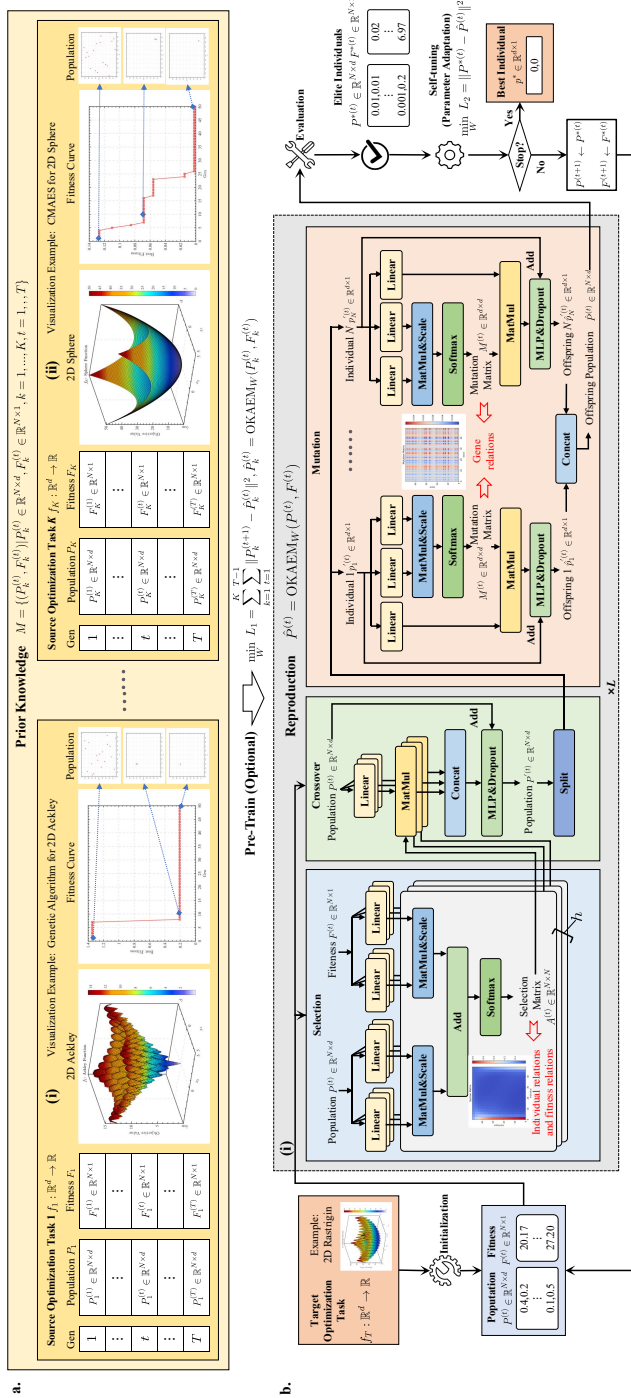


Fig. 1 Schematic flow of OKAEM. a. Pre-training on prior knowledge (optional); (i) example: prior knowledge accumulated using a genetic algorithm on the 2D-Ackley problem; (ii) example: prior knowledge accumulated using CMAES on the 2D-Sphere problem. b. Adaptive optimization to solve target tasks. This phase includes initialization, reproduction, evaluation, elitism, and self-tuning (parameter adaptation): (i) selection, crossover, and mutation modules used in reproduction.

elite individuals. The novel combination of pre-training and self-tuning mechanisms addresses the inflexibility of existing customized LEAs. Notably, even without prior knowledge, users can still execute the adaptive optimization phase to effectively solve target tasks.

Experimental results show that OKAEM significantly outperforms classical and advanced EKT methods across 12 transfer scenarios with varying similarities, highlighting the efficient use of prior knowledge. Without prior knowledge (no pre-training), OKAEM still achieves competitive performance on 24 black-box optimization problems compared to state-of-the-art LEAs, thanks to its self-tuning capabilities. Leveraging parallel computing, OKAEM requires only a few GPU seconds. In a practical case study on prompt tuning for vision-language models, OKAEM surpasses state-of-the-art black-box baselines. Moreover, we find that OKAEM improves its performance with knowledge accumulation and explicitly learns the principles of natural selection and genetic recombination.

2 Optimization knowledge adaptation evolutionary model

We consider applying optimization knowledge to EAs to find the optimal solution of a complex non-analytic function: $\min_x [f(x) \mid M, P]$, where $f \in \mathbb{R}^1$ is the objective function, and $x \in \mathbb{R}^d$ is the decision variable. $M = \{(P_k^{(t)}, F_k^{(t)}) \mid P_k^{(t)} \in \mathbb{R}^{N \times d}, F_k^{(t)} \in \mathbb{R}^{N \times 1}, k = 1, \dots, K, t = 1, \dots, T\}$ represents a series of prior knowledge accumulated from source tasks. $P_k^{(t)}$ and $F_k^{(t)}$ denote the population and fitness data of the k -th source task at generation t . Each individual in the population represents a candidate solution for the optimization task. Fig. 1a visualizes the prior knowledge M accumulated by GA and CMAES on two 2D source optimization tasks: Ackley and Sphere. These visualizations intuitively reflect the evolutionary behaviors of populations on the source tasks. $P = \{(P^{(t)}, F^{(t)}) \mid P^{(t)} \in \mathbb{R}^{N \times d}, F^{(t)} \in \mathbb{R}^{N \times 1}, t = 1, \dots, j\}$ denotes the optimization knowledge accumulated from the 1st to the j -th generation on the target task. The proposed OKAEM includes two stages: 1) pre-training on M (Fig. 1a); adaptive optimization using P (Fig. 1b). For the pseudocode of OKAEM, see Supplementary Appendix A.

2.1 Architecture

Given the current population $P^{(t)} \in \mathbb{R}^{N \times d}$ and fitness data $F^{(t)} \in \mathbb{R}^{N \times 1}$, OKAEM generates an offspring population $\hat{P}^{(t)} \in \mathbb{R}^{N \times d}$ through selection, crossover, and mutation, denoted as $\hat{P}^{(t)} = \text{OKAEM}_W(P^{(t)}, F^{(t)})$ (Fig. 1 b(i)). The selection module defines a selection matrix $A^{(t)} \in \mathbb{R}^{N \times N}$, where A_{ij} indicates individual j 's contribution to generating the i -th individual for crossover. Multi-head attention mechanisms [31] parameterize $A^{(t)}$ to model individual and fitness relationships. Using $A^{(t)}$, the crossover module recombines individuals in $P^{(t)}$ to produce an intermediate population $P'^{(t)}$. In addition, an MLP with Dropout is employed to ensure the randomness of the crossover operator. The mutation module perturbs each $p_i^{(t)} \in \mathbb{R}^{d \times 1}$ in $P'^{(t)}$ to generate the corresponding offspring $\hat{p}_i^{(t)} \in \mathbb{R}^{d \times 1}$. A mutation matrix $M^{(t)} \in \mathbb{R}^{d \times d}$,

where M_{jk} indicates the influence of the k -th gene on the mutation of the j -th gene, is parameterized using attention mechanisms to model gene interactions. By applying $M^{(t)}$ to each individual $p_i^{(t)}$, we introduce gene-level perturbations to generate each offspring $\hat{p}_i^{(t)}$. Collectively, these offspring form the offspring population $\hat{P}^{(t)}$. For detailed information on each component, see Methods 4.

Compared with traditional EAs, OKAEM offers three key advantages: learnability, parallelizability, and interpretability.

- **Learnability:** The parameterized selection, crossover, and mutation modules can be adaptively updated based on optimization knowledge, rather than relying on heuristic rules. This adaptive learning capability enhances the generalization performance.
- **Parallelizability:** By adhering to the fundamental design principles of neural networks, OKAEM enables the direct application of existing GPU-based parallel computing strategies. This significantly reduces computational costs and accelerates the optimization process.
- **Interpretability:** OKAEM allows for the visualization of the selection and mutation matrices, providing valuable insights into individual relationships, fitness dynamics, and gene interactions during the evolutionary process. Specifically, observations from these visualizations reveal distinct statistical patterns: individuals with higher fitness are more likely to be selected for crossover, and gene mutations exhibit consistent patterns. For a detailed analysis of these advantages, see Fig 3.

2.2 Pre-training and adaptive optimization

The pre-training aims to uncover the patterns underlying prior knowledge to enhance the performance of OKAEM. As shown in Fig. 1a, given prior knowledge M , the optimization objective of pre-training is to minimize the Euclidean distance between the predicted offspring population $\hat{P}_k^{(t)}$ and the actual next-generation population $P_k^{(t+1)}$ in the prior knowledge:

$$\min_W L_1 = \sum_{k=1}^K \sum_{t=1}^{T-1} \|P_k^{(t+1)} - \hat{P}_k^{(t)}\|^2, \quad \hat{P}_k^{(t)} = \text{OKAEM}_W(P_k^{(t)}, F_k^{(t)}). \quad (1)$$

This allows OKAEM to explicitly learn population evolution behavior by predicting the next generation. Traditional EKT methods rely on heuristic rules to determine what, when, and how to transfer knowledge, focusing only on a subset of promising prior knowledge and heavily depending on expert design [14, 21]. In contrast, OKAEM utilizes all prior knowledge for pre-training, avoiding knowledge waste. Moreover, prior knowledge generated by different EAs on a set of source optimization tasks can be used as training data, enabling OKAEM to learn diverse types of evolution behaviors (see detailed analysis in Fig. 2b).

As shown in Fig. 1b, adaptive optimization comprises initialization, reproduction, evaluation, elitism, and self-tuning. Over T generations, the best individual $p^* \in \mathbb{R}^d$ is obtained. Initially, Latin hypercube sampling is used to generate a random initial

population from the search space. By leveraging the pre-trained OKAEM, we proceed with population reproduction. Subsequently, the offspring population undergoes fitness evaluation. Furthermore, an elitism strategy ensures that the top N individuals with the highest fitness are carried over to the next generation. Finally, self-tuning updates OKAEM’s parameters by minimizing the distance between the generated offspring population $\hat{P}^{(t)}$ and the elite individuals $P^{*(t)}$:

$$\min_W L_2 = \|P^{*(t)} - \hat{P}^{(t)}\|^2. \quad (2)$$

During the self-tuning phase, OKAEM iteratively updates its parameters to adapt to the current target task. From a learning perspective, pre-training and self-tuning correspond to unsupervised and supervised learning paradigms, respectively. We can use classical gradient optimizers such as AdamW [32] to update the model parameters W . Pre-training aims to more comprehensively utilize prior knowledge (transferability), while self-tuning aims to learn new knowledge generated by itself (adaptability). These processes leverage population dynamics and fitness evaluations, independent of explicit gradient information from the fitness function, providing a robust training strategy for EAs. Furthermore, the modular design of pre-training and self-tuning ensures effectiveness even without prior knowledge, enabling direct adaptive optimization on the target task. This dual-phase approach enhances OKAEM’s ability to generalize and adapt, making it suitable for a wide range of optimization challenges.

3 Results

3.1 Sequence transfer optimization problem

We evaluate OKAEM’s performance on the sequence transfer optimization problem (STOP) suite [33], a comprehensive benchmark comprising 12 problems that simulate knowledge transfer scenarios in EAs. Each STOP task encompasses a target task and prior knowledge derived from a set of source optimization tasks, effectively representing the spectrum of similarity relationships between optimal solutions encountered in real-world applications. The problems are categorized into three groups based on their degree of similarity: high (STOP1-4), mixed (STOP5-8), and low (STOP9-12). The baselines include both classical and advanced EKT methods [21], encompassing various dimensions of knowledge transfer: non-transfer strategies (N), what to transfer (H, M1, WD, OC, ROC, KLD), how to transfer (M1-Te, M1-Tr, M1-Tm, M1-M, M2-A, OC-L, OC-A, OC-K, OC-N, ROC-L), and when to transfer (F-1, F-5, F-10, D-M, D-P, and D-G). Additionally, two variants of OKAEM serve as baselines for comparison: OKAEM-PT, which relies solely on pre-training, and OKAEM-ST, which focuses exclusively on self-tuning. This setup allows us to comprehensively assess the effectiveness of OKAEM’s dual-phase approach in leveraging prior knowledge and adapting to new tasks. For detailed problem configurations and parameter settings, see Supplementary Appendix B.

As shown in Fig. 2a, the experimental results provide several key insights:

- **Resilience in low similarity:** Most EKT methods perform worse than non-transfer approaches in low-similarity scenarios (STOP9-12) due to limited shared knowledge and negative transfer [21]. Notably, OKAEM excels even under these challenging conditions. Pre-training on low-similarity source tasks improves model generalizability, leading to superior target task performance.
- **Importance of pre-training and self-tuning:** In all transfer scenarios, OKAEM outperforms both OKAEM-ST and OKAEM-PT, highlighting the critical role of integrating both pre-training and self-tuning phases in enhancing overall performance.
- **Enhanced optimization by self-tuning:** OKAEM significantly surpasses OKAEM-ST, with the key difference being the execution of self-tuning during the optimization phase. This finding indicates that parameter adaptation allows OKAEM to continuously improve its optimization performance as new knowledge accumulates.

These results collectively demonstrate OKAEM’s robustness and adaptability across diverse knowledge transfer scenarios, validating its effectiveness in leveraging prior knowledge for enhanced EAs.

OKAEM exhibits the capability to learn from different types of prior knowledge. For each STOP, we generate diverse prior knowledge using GA [2], particle swarm optimization (PSO) [34], and CMAES [25] on source tasks, respectively. Detailed parameter settings are provided in Supplementary Appendix B. Fig. 2b illustrates the performance comparison between OKAEM, trained with different types of prior knowledge, and the corresponding source algorithms on target tasks. In all cases, OKAEM outperforms the source algorithms, indicating its capability to leverage various types of prior knowledge to enhance optimization efficiency. This robust performance gain highlights OKAEM’s adaptability and versatility in enhancing optimization outcomes using different strategies.

We visualize the selection and mutation matrices learned by OKAEM for STOP1, STOP5, and STOP9 (Fig. 3). Across all cases, these matrices exhibit clear statistical patterns. For the selection matrix, individuals with higher fitness values are preferentially selected, embodying the principle of “survival of the fittest”. Notably, individuals with the lowest fitness are selected more frequently than those with mid-range fitness, likely to maintain population diversity. The mutation matrix evolves from random to ordered over generations, exhibiting “row-similarity” characteristics, which indicate consistent patterns in gene variation. This evolution enhances the interpretability of our method compared to existing LEAs. In addition, ablation studies (Supplementary Table B5) show that eliminating either the crossover or mutation mechanisms results in a substantial performance drop, highlighting their indispensable roles in driving OKAEM’s superior performance.

3.2 Black-box optimization benchmark problem

In many practical scenarios, collecting prior knowledge can be challenging, rendering pre-training infeasible. Leveraging its flexibility, OKAEM can perform adaptive optimization independently to solve complex tasks. This section evaluates OKAEM’s

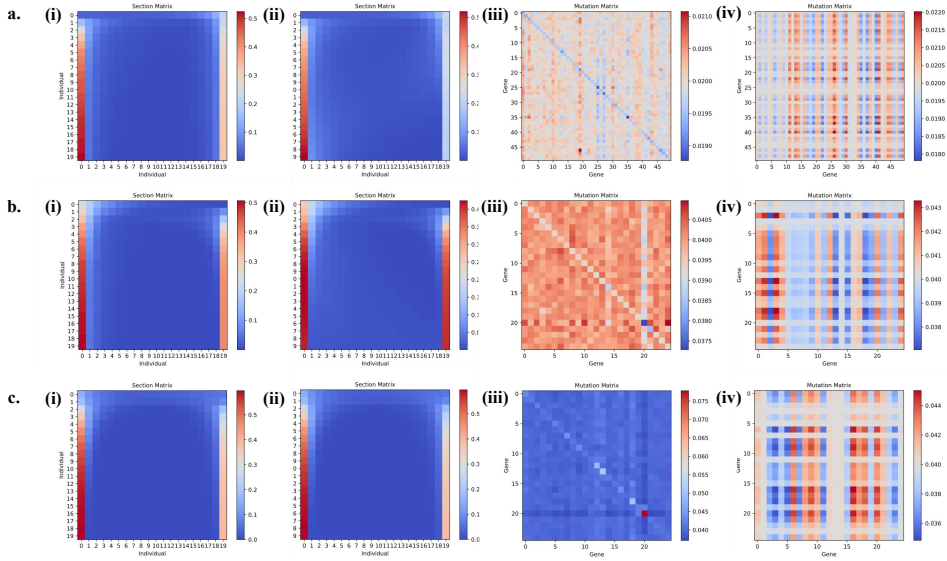


Fig. 3 Visualization of selection and mutation matrices learned by OKAEM on STOP1, STOP5, and STOP9. For the selection matrix, axes represent individuals ranked by their fitness scores, with 0 and 19 denoting the best and worst individuals, respectively. The matrix values are computed as the mean across all H attention heads. For the mutation matrix, axes represent gene (decision variable) indices. a. STOP1: (i)-(ii) First and T -th generation selection matrices; (iii)-(iv) First and T -th generation mutation matrices. b. STOP5: (i)-(ii) First and T -th generation selection matrices; (iii)-(iv) First and T -th generation mutation matrices. c. STOP9: (i)-(ii) First and T -th generation selection matrices; (iii)-(iv) First and T -th generation mutation matrices.

performance without pre-training on 24 commonly used black-box optimization benchmarks (BBOBs) [35, 36], with a search space of $[-10, 10]^d$ where $d = 1000$. The BBOB suite encompasses a series of high-dimensional continuous optimization functions, including unimodal, multimodal, rotated, and shifted functions, as well as those with specific properties such as Lipschitz continuity and second-order differentiability. We compare OKAEM against both classical adaptive EAs and advanced learnable EAs, including SimpleGA [37], GESMR-GA [38], XNES [39], CMAES [25], LGA [26], and LES [27]. All algorithms are implemented using JAX [40] for its acceleration benefits. Detailed descriptions of the comparison baselines and parameter settings are provided in Supplementary Appendix C.

As observed in Fig. 4a, OKAEM achieves superior performance across most benchmarks, regardless of their diverse geometric properties. This indicates that even without prior knowledge (i.e., pre-training), OKAEM’s adaptive optimization can deliver highly competitive results. Unlike classical adaptive algorithms such as GESMR, XNES, and CMAES, which rely on specific structures of evolutionary operators, OKAEM’s parameter adaptation is entirely driven by population dynamics and fitness. This flexibility makes it suitable for any neural representation-based evolutionary operator. By adjusting its parameters based on population dynamics, OKAEM outperforms all baselines, demonstrating strong adaptability and optimization capabilities. Conversely, LGA and LES rely on fixed parameters post-training,

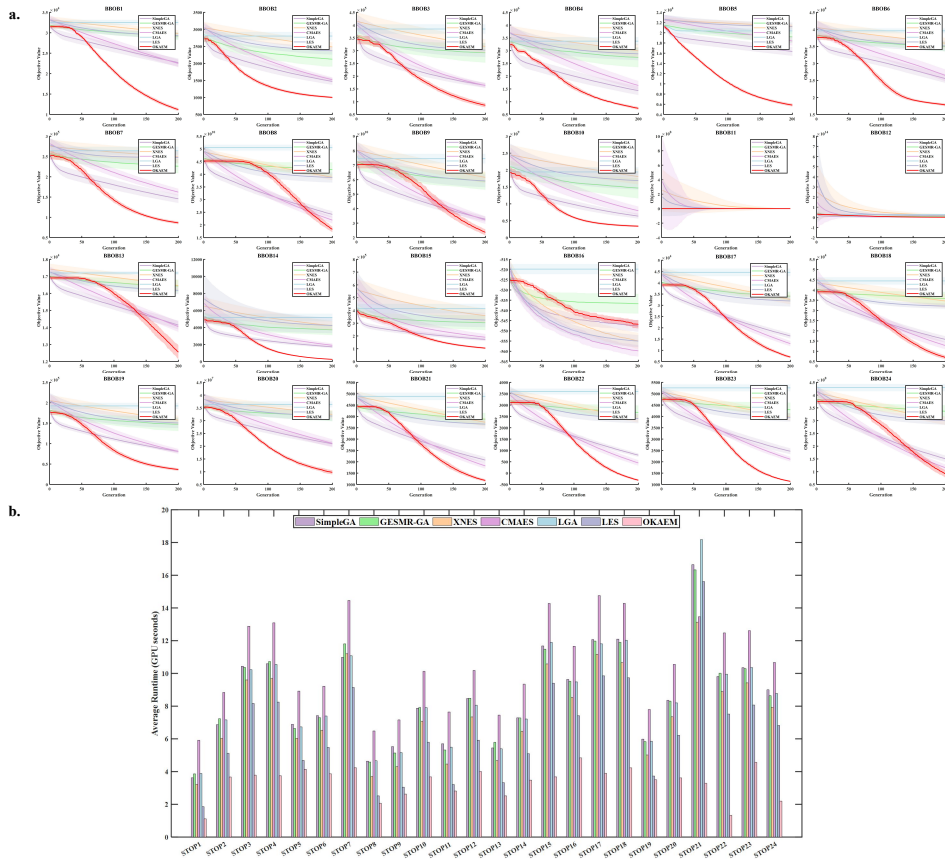


Fig. 4 Experimental results on 24 BBOB Benchmarks (20 independent runs with random initialization, population size $N = 20$, number of iterations $T = 200$). a. Average convergence curves. b. Average GPU runtime. For more detailed performance comparisons, see Supplementary Fig. C1.

preventing them from adapting to population changes. As demonstrated by OKAEM’s outstanding results, adaptability is crucial for enhancing the performance of EAs. Moreover, Fig. 4b shows that OKAEM has the lowest computational cost among all baselines, requiring only a few GPU seconds. This indicates that neural representation-based OKAEM can significantly enhance computational efficiency through parallel computing.

3.3 Black-box prompt tuning for the vision-language model

Pre-trained models, particularly those for vision-language tasks, are commonly released as services that allow users to set task-specific prompts to query the models [41]. EAs such as CMAES are widely used to optimize these prompts to enhance the performance of pre-trained models [41–44]. Without access to the model’s architecture or gradient information, optimizing prompts in this black-box setting remains a significant challenge. Let the forward propagation of a vision-language model be denoted

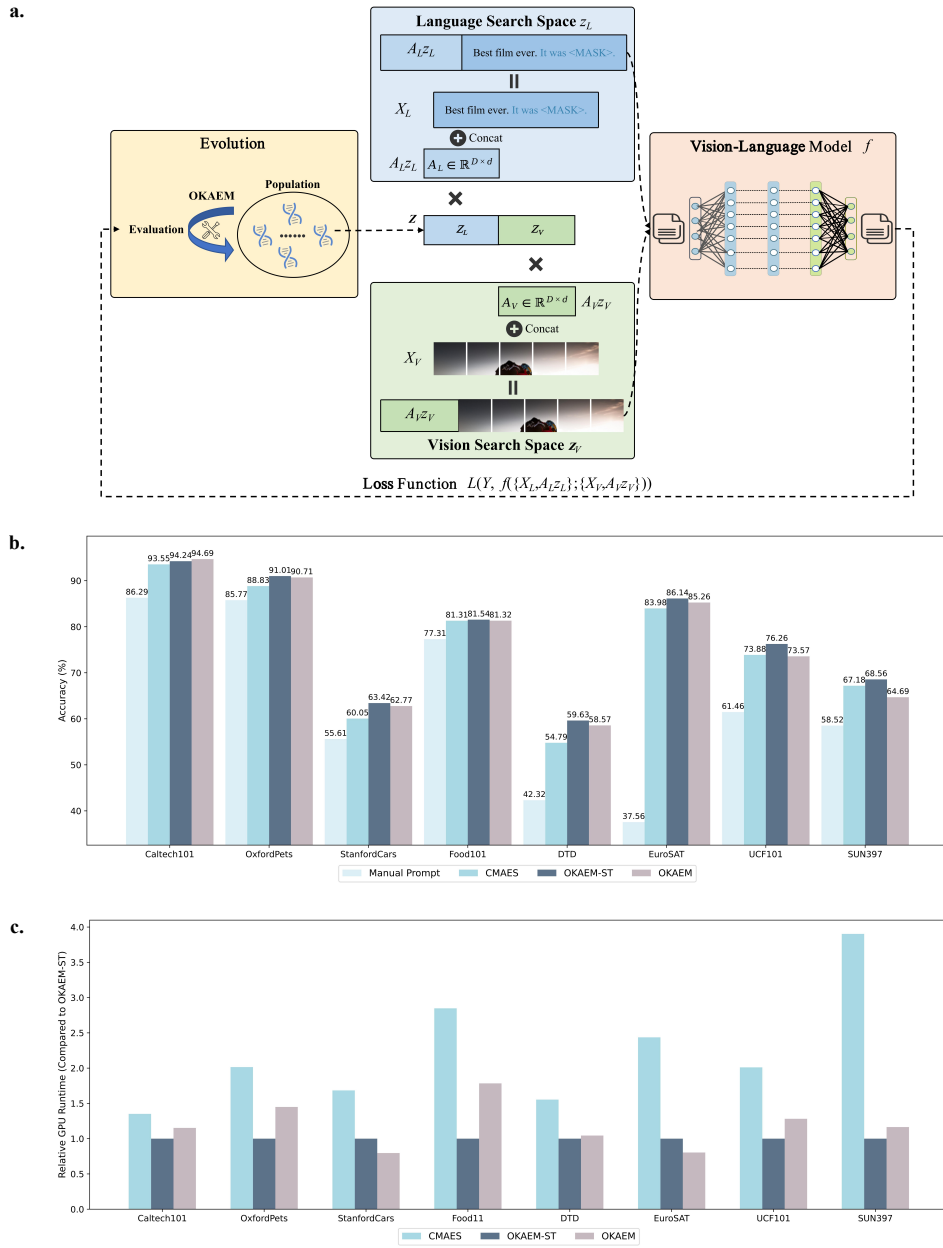


Fig. 5 Black-box prompt tuning for vision-language models. a. Illustration of the prompt tuning process. b. Average test accuracies on 8 common visual image classification tasks over five independent runs. c. Relative GPU runtime of the automatic tuning methods compared to OKAEM-ST.

as f . Given batches of texts X_L and images X_V , along with respective text prompts p_L and image prompts p_V , the model outputs a similarity score for each image-text pair. As shown in Fig. 5a, with outputs and labels Y , the objective of prompt tuning is to minimize the cross-entropy loss L :

$$Z^* = \arg \min_{Z=\{z_L, z_V\}} L(Y, f(\{X_L, p_L\}; \{X_V, p_V\})), \quad (3)$$

where

$$p_L = A_L Z_L, \quad p_V = A_V Z_V,$$

and Z represents the parameter subspace for prompts to be optimized, composed of the text intrinsic vector Z_L and visual intrinsic vector Z_V . The randomly initialized fixed matrices A_L and A_V project Z_L and Z_V into the text prompt p_L and image prompt p_V , respectively. This optimization objective is computed using only the forward pass of the vision-language model, eliminating the need for backpropagation.

To validate OKAEM’s capability to solve complex real-world problems, we evaluate its performance on eight commonly used visual image classification datasets (see Fig. 5b): Caltech101 [45], OxfordPets [46], StanfordCars [47], Food101 [48], UCF101 [49], SUN397 [50], EuroSAT [51], and DTD [52]. We compare OKAEM against three types of methods: 1) Manually designed prompts [53], which use carefully crafted templates for zero-shot evaluation. 2) CMAES [41, 44], a state-of-the-art black-box tuning algorithm widely used for optimizing prompts in pre-trained models. 3) OKAEM-ST, a variant of OKAEM that performs only adaptive optimization without pre-training. Additionally, we employ CMA-ES for prompt tuning on the Caltech101 dataset to generate prior knowledge for pre-training OKAEM. Once trained, OKAEM directly tunes prompts across all datasets without separate pre-training for each one. Detailed experimental setups are provided in Supplementary Appendix D.

Fig. 5b illustrates that black-box tuning methods consistently outperform manual prompting, underscoring the importance and efficacy of automated tuning. After multiple function evaluations, OKAEM-ST achieves higher accuracy on most datasets compared to the baselines. Notably, OKAEM demonstrates an advantage over OKAEM-ST on the Caltech101 dataset. This is attributed to the prior knowledge derived from Caltech101, highlighting the improvement in model performance when the prior knowledge closely aligns with the target task. Moreover, Fig. 5c shows that both OKAEM and OKAEM-ST exhibit lower computational costs compared to CMAES, significantly accelerating evolutionary computation in practical applications.

3.4 Parameter sensitivity analysis

Fig. 6 presents the sensitivity analysis of OKAEM’s four critical parameters on the STOP suite: the number of layers L , population size N , dropout probability p_C in crossover, and dropout probability p_M in mutation. Fig. 6a illustrates that the performance of OKAEM improves with an increase in both the number of source tasks and model depth, regardless of whether the task similarity is high (STOP1-STOP4) or low (STOP9-STOP12). More source tasks provide richer prior knowledge, allowing deeper models to capture complex patterns. The positive correlation between

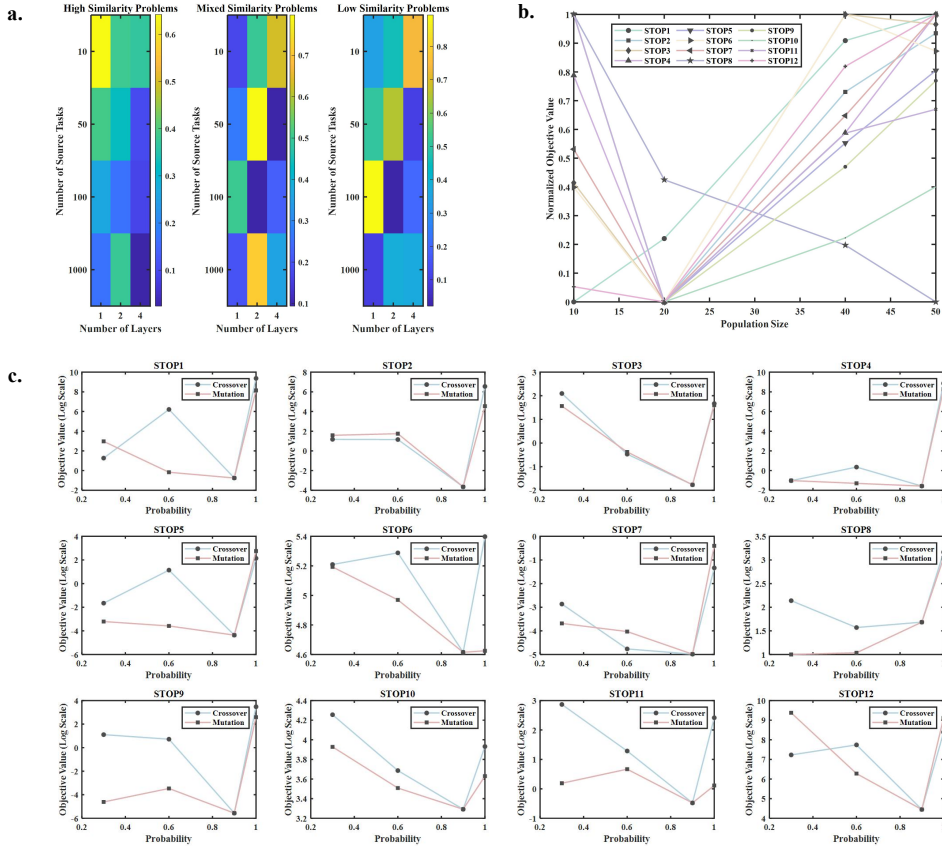


Fig. 6 Sensitivity analysis of key parameters in OKAEM (20 independent runs with random initialization). The stopping criterion is set to a maximum of 5000 evaluations. a. Analysis of layers $L \in [1, 2, 4]$ and number of source tasks $K \in [10, 50, 100, 1000]$. The heatmap displays the average normalized objective values across different types of STOP, with all values scaled to the $[0, 1]$ using min-max normalization. b. Population size $N \in [10, 20, 40, 50]$. The y-axis shows the normalized objective values. c. Dropout probability $p_C \in [0.3, 0.6, 0.9, 1]$ in crossover and dropout probability $p_M \in [0.3, 0.6, 0.9, 1]$ in mutation. The x-axis represents the objective values on a log scale.

performance and prior knowledge is especially pronounced in highly similar contexts (STOP1-STOP4). This implies that OKAEM’s optimization capacity strengthens with the accumulation of prior knowledge. Conversely, in mixed-similarity conditions (STOP5-STOP8), the relationship between source tasks, model depth, and performance becomes more complex. For these cases, we recommend manually tuning the model depth for optimal results.

As indicated in Fig. 6b, a population size of 20 is recommended when the maximum number of evaluations is 5000. In practice, the population size should be adjusted based on the problem dimensions. Fig. 6c illustrates that initial increases in p_C and p_M improve the performance of OKAEM. However, performance degrades when these parameters exceed critical thresholds. Specifically, setting p_C or p_M to 1 eliminates randomness in crossover or mutation, leading to suboptimal performance. Based on

experimental results, we recommend using moderately high values for p_C and p_M to balance performance optimization and stability.

4 Methods

4.1 Implementation details of OKAEM

4.1.1 Selection

We employ attention mechanisms to model individual and fitness relations, parameterizing the selection module. Given the current population $P^{(t)} \in \mathbb{R}^{N \times d}$ and fitness $F^{(t)} \in \mathbb{R}^{N \times 1}$, the selection matrix $A^{(t)} \in \mathbb{R}^{N \times N}$ is defined as follows:

$$A^{(t)} = \text{softmax} \left(\frac{A_P^{(t)} + A_F^{(t)}}{\sqrt{d_A}} \right), \quad (4)$$

where

$$A_P^{(t)} = (P^{(t)}W^{QP})(P^{(t)}W^{KP})^T, A_F^{(t)} = (F^{(t)}W^{QF})(F^{(t)}W^{KF})^T.$$

$A_P^{(t)}$ captures pairwise interactions between individuals in the population, while $A_F^{(t)}$ models the interplay between their fitness scores. The matrices $W^{QP}, W^{KP} \in \mathbb{R}^{d \times d_A}$ and $W^{QF}, W^{KF} \in \mathbb{R}^{1 \times d_A}$ are learnable parameters that transform the original features into a space conducive to learning the selection policy. The softmax function converts the relation scores into a probability distribution, scaled by $\sqrt{d_A}$ to stabilize optimization and prevent gradient explosion. Element $A_{ij}^{(t)}$ in the selection matrix can be used to quantify the extent to which individual j influences the generation of individual i by crossover.

4.1.2 Crossover

The crossover module begins by applying the selection matrix $A^{(t)}$ to the current population $P^{(t)}$ for individual-level recombination:

$$O_C^{(t)} = A^{(t)}P^{(t)}W^V, \quad (5)$$

where the transformation $W^V \in \mathbb{R}^{d \times d_A}$ reduces the dimensionality of the search space. This dimensionality reduction is a well-established technique in EAs to enhance optimization efficiency and reduce computational complexity [54, 55].

To enhance the expressiveness of the crossover, we employ multi-head attention mechanisms that focus on the features of the population and fitness across different subspaces. Given H heads, Eq. (5) becomes:

$$O_C^{(t)} = \parallel_{h=1}^H A_h^{(t)} P^{(t)} W_h^V, \quad (6)$$

where

$$A_h^{(t)} = \text{Softmax} \left(\frac{(P^{(t)}W_h^{QP})(P^{(t)}W_h^{KP})^T + (F^{(t)}W_h^{QF})(F^{(t)}W_h^{KF})^T}{\sqrt{d_A/H}} \right),$$

and $W_h^V, W_h^{QP}, W_h^{KP} \in \mathbb{R}^{d \times (d_A/H)}$, $W_h^{QF}, W_h^{KF} \in \mathbb{R}^{1 \times (d_A/H)}$.

Next, we introduce nonlinearity into $O_C^{(t)}$ using a MLP with Dropout:

$$MLP(O_C^{(t)}) = \text{Dropout}_{p_C}(\text{Tanh}(O_C^{(t)}W_1 + b_1))W_2 + b_2, \quad (7)$$

where $\text{Tanh}()$ is the activation function, and $W_1 \in \mathbb{R}^{d_A \times d_M}$, $b_1 \in \mathbb{R}^{d_M}$, $W_2 \in \mathbb{R}^{d_M \times d}$, $b_2 \in \mathbb{R}^d$ are parameters. The Dropout introduces stochasticity, with probability p_C controlling neuron deactivation, thereby modulating the randomness of the crossover process. Finally, residual connections are used to generate the post-crossover intermediate population:

$$P'^{(t)} = P^{(t)} + MLP(O_C^{(t)}), \quad (8)$$

which helps mitigate gradient vanishing during training, ensuring stable convergence.

In summary, the learnable parameters W_{SC} for the selection and crossover modules are:

$$W_{SC} = \{W_h^{QP}, W_h^{KP}, W_h^{QF}, W_h^{KF}, W_h^V, W_1, b_1, W_2, b_2, h = 1, \dots, H\}. \quad (9)$$

4.1.3 Mutation

The mutation module individually perturbs each individual $p_i^{(t)} \in \mathbb{R}^{d \times 1}$ in the intermediate population $P'^{(t)}$ to generate the corresponding offspring $\hat{p}_i^{(t)} \in \mathbb{R}^{d \times 1}$. Employing attention mechanisms, we model gene relations to guide the mutation process. The mutation matrix $M^{(t)} \in \mathbb{R}^{d \times d}$ is defined as:

$$M^{(t)} = \text{Softmax} \left(\frac{(p_i^{(t)}W^{QM})(p_i^{(t)}W^{KM})^T}{\sqrt{d_A}} \right), \quad (10)$$

where $W^{QM}, W^{KM} \in \mathbb{R}^{1 \times d_A}$. Similar to the crossover module, we use residual connections and a MLP to generate offspring:

$$\hat{p}_i^{(t)} = p_i^{(t)} + MLP(O_M^{(t)}), \quad (11)$$

with

$$O_M^{(t)} = M^{(t)}p_i^{(t)}W^{VM}, \quad (12)$$

and

$$MLP(O_M^{(t)}) = \text{Dropout}_{p_M}(\text{Tanh}(O_M^{(t)}W_3 + b_3))W_4 + b_4, \quad (13)$$

where $W^{VM} \in \mathbb{R}^{1 \times d_A}$, $W_3 \in \mathbb{R}^{d_A \times d_M}$, $b_3 \in \mathbb{R}^{d_M}$, $W_4 \in \mathbb{R}^{d_M \times 1}$, and $b_4 \in \mathbb{R}^1$. The Dropout layer with probability p_M introduces stochasticity into the mutation process.

All generated offspring are then combined into the offspring population $\hat{P}(t) \in \mathbb{R}^{N \times d}$:

$$\hat{P}(t) = \parallel_{i=1}^N (\hat{p}_i^{(t)})^T. \quad (14)$$

The parameters of the mutation module are summarized as:

$$W_M = \{W^{QM}, W^{KM}, W^{VM}, W_3, b_3, W_4, b_4\}. \quad (15)$$

In summary, the learnable parameters W of a single layer of OKAEM include all weight matrices and bias vectors from the selection, crossover, and mutation:

$$\begin{aligned} W &= \{W_{SC}, W_M\} \\ &= \{W_h^{QP}, W_h^{KP}, W_h^{QF}, W_h^{KF}, W_h^V, W_1, b_1, W_2, b_2, \\ &\quad W^{QM}, W^{KM}, W^{VM}, W_3, b_3, W_4, b_4, h = 1, \dots, H\}. \end{aligned} \quad (16)$$

4.2 Computational complexity analysis

The selection matrix and the MLP primarily determine the computational complexity of the selection and crossover. According to Eq. (4), the complexity of computing the selection matrix is $O(N \cdot d \cdot d_A + N^2 \cdot d_A)$, where N is the population size, d is the dimensionality of the search space, and d_A is the embedding dimension. From Eq. (7), the complexity of the MLP involved in the crossover is $O(N \cdot d_A \cdot d_M + N \cdot d_M \cdot d)$, with d_M representing the hidden layer dimension. Therefore, the total complexity for selection and crossover is $O(N \cdot d \cdot d_A + N^2 \cdot d_A + N \cdot d_A \cdot d_M + N \cdot d_M \cdot d)$.

According to Eq. (10), the complexity of computing the mutation matrix is $O(d \cdot d_A + d^2 \cdot d_A)$. Eq. (13) indicates that the MLP involved in mutation has a complexity of $O(d \cdot d_A \cdot d_M)$. Thus, the overall complexity for mutation is: $O(d^2 \cdot d_A + d \cdot d_A \cdot d_M)$.

Consolidating these results, the total computational complexity for an L -layer architecture is $O(L \cdot N \cdot d \cdot d_A + L \cdot N^2 \cdot d_A + L \cdot N \cdot d_A \cdot d_M + L \cdot N \cdot d_M \cdot d + L \cdot d^2 \cdot d_A + L \cdot d \cdot d_A \cdot d_M)$. Assuming $d_A = d_M = d$, this simplifies to $O(L \cdot N \cdot d^2 + L \cdot N^2 \cdot d + L \cdot d^3)$. In complex optimization scenarios, where the population size N is generally smaller than the problem dimension d , the leading term of complexity is $O(L \cdot d^3)$. This highlights the significant impact of the problem dimension d on computational requirements in high-dimensional search spaces. The assumption $d_A = d_M = d$ simplifies the analysis but may not hold in practice. Careful consideration should be given to the specific values of d_A and d_M based on the application context.

5 Discussion

With the advancement in computational capabilities, complex optimization tasks in scientific and industrial fields have become increasingly intricate and challenging. Traditional EAs often rely heavily on specific problem structures, limiting their ability to leverage the vast amount of valuable knowledge generated during optimization. This constrained transferability and adaptability hinder their optimization performance and reduce confidence in practical applications. This paper introduces a novel neural representation-based evolutionary framework, OKAEM, which efficiently utilizes prior knowledge and quickly adapts to self-generated new knowledge. As demonstrated on 12 STOPS, 24 BBOBs, and a real-world case study, OKAEM exhibits superior optimization performance compared to existing baselines, thanks to its robust transferability and adaptability. Extensive experiments show that OKAEM exhibits strong learnability: 1) Its optimization capability improves as knowledge accumulates; 2) It can explicitly learn the principles of natural selection and genetic combination

in evolution. Thus, OKAEM takes a significant step forward in modeling transferability, adaptability, and learnability in EAs, overcoming the inflexibility of existing customized methods and providing a foundational model for addressing larger-scale complex optimization tasks.

Despite the notable progress made by OKAEM, several avenues for improvement remain. Experimental results (Fig. 2a) show that in certain mixed-similarity scenarios (STOP6 and STOP8), OKAEM outperforms methods without knowledge transfer but falls short of those specifically designed for "what-to-transfer". This highlights the potential benefits of refining pre-training datasets to better match target tasks. Integrating end-to-end training with fitness evaluation environments could enhance OKAEM's performance in real-world applications by leveraging the synergy between evolution and evaluation. Additionally, the current framework is not tailored for multi-objective optimization, a common application area for EAs [56, 57]. Constructing prior knowledge, model architectures, and training paradigms for multi-objective optimization merits further exploration. Selecting foundational source optimization tasks when constructing prior knowledge datasets can significantly improve model generalization, potentially leading to large-scale pre-trained models capable of addressing diverse optimization challenges. Moreover, A rigorous convergence analysis of OKAEM is crucial for establishing theoretical guarantees. Developing more advanced neural representation-based evolutionary operators, especially those with rotary position embedding [58], promises to reduce computational complexity. It should be noted that these challenges present engineering opportunities rather than insurmountable barriers.

Data availability

The implementations of STOPS and BBOBs are publicly available. STOPS can be accessed at <https://github.com/XmingHsueh/STOP-G>, while the BBOB implementation is provided at <https://numbbo.github.io/coco/testsuites/bbob>. In addition, the prompt tuning for visual-language models is detailed in <https://github.com/BruthYU/BPT-VLM>.

Code availability

The Python implementation of OKAEM is available at <https://github.com/xiaofangxd/OKAEM>. Matlab codes for EKT methods can be found at <https://github.com/XmingHsueh/STO-EC>. Additionally, the Python code for all comparison baselines used in the BBOB experiments is provided at <https://github.com/RobertTLange/evosax>.

Appendix A Pseudocode of OKAEM

The pseudocode of OKAEM is shown in Algorithm 1.

Algorithm 1 Optimization knowledge adaptation evolutionary model

Require:

- Optimization task $\min_{x \in X} f(x)$, $X \in \mathbb{R}^d$;
- Prior knowledge $M = \{(P_k^{(t)}, F_k^{(t)}) \mid P_k^{(t)} \in \mathbb{R}^{N \times d}, F_k^{(t)} \in \mathbb{R}^{N \times 1}, k = 1, \dots, K, t = 1, \dots, T\}$ (Optional);
- Pre-training loss L_1 (Optional);
- Self-tuning loss L_2 ;
- Architecture parameters: number of layers L , embedding dimension d_A , attention heads H , MLP hidden dimension d_M , dropout probability in crossover p_C , dropout probability in mutation p_M ;
- Training parameters: learning rate lr , weight decay wd ;
- Evolutionary parameters: population size N , number of iterations T .

Ensure:

- Optimal individual $p^* \in \mathbb{R}^d$.
 - 1: $\text{OKAEM}_W \leftarrow \text{Initialization}(L, d_A, H, d_M, p_C, p_M)$; \triangleright Initialize the model
 - 2: $W^{(0)} \leftarrow \text{AdamW}(L_1(M), lr, wd)$; \triangleright Pre-train using AdamW with loss L_1 (Optional)
 - 3: $P^{(0)} \in \mathbb{R}^{N \times d} \leftarrow \text{LHSampling}(X)$; \triangleright Initialize the population using Latin hypercube sampling
 - 4: $F^{(0)} \in \mathbb{R}^N \leftarrow f(P^{(0)})$; \triangleright Evaluate the fitness based on the optimization task
 - 5: **for** $t = 0$ to T **do**
 - 6: $\hat{P}^{(t)} \leftarrow \text{OKAEM}_{W^{(t)}}(P^{(t)}, F^{(t)})$; \triangleright Reproduce using $\text{OKAEM}_{W^{(t)}}$
 - 7: $\hat{F}^{(t)} \leftarrow f(\hat{P}^{(t)})$; \triangleright Evaluate the fitness based on the optimization task
 - 8: $P^{*(t)}, F^{*(t)} \leftarrow \text{Elitism}(P^{(t)} \cup \hat{P}^{(t)}, F^{(t)} \cup \hat{F}^{(t)})$; \triangleright Select top N individuals based on fitness
 - 9: $W^{(t)} \leftarrow \text{AdamW}(L_2(\hat{P}^{(t)}, P^{*(t)}), lr, wd)$; \triangleright Self-tune using AdamW with loss L_2
 - 10: $P^{(t+1)}, F^{(t+1)} \leftarrow P^{*(t)}, F^{*(t)}$; \triangleright Update the population and fitness
 - 11: **end for**
 - 12: $p^* \leftarrow \text{Selection}(P^{(T)}, F^{(T)})$; \triangleright Select the best individual from the final population
-

Appendix B Sequence transfer optimization problem

B.1 Problem configuration

The test suite consists of 12 sequential transfer optimization problems (STOPs), each featuring a set of source optimization tasks and a target optimization task [33]. The goal is to leverage knowledge acquired from the source tasks to improve performance on the target task. As detailed in Supplementary Table B1, each STOP is configured using six parameters: task family, transfer scenario, similarity distribution, task dimensionality, number of source tasks, and source optimization algorithm.

Table B1 Candidate configurations for STOP parameters.

Parameter	Candidate configurations
Task family γ	$\{f_1, f_2, f_3, f_4, f_5, f_6, f_7, f_8\}$
Transfer scenario T	$\{T_a, T_e\}$
Similarity distribution h	$\{h_1^h, h_2^h, h_1^m, h_2^m, h_3^m, h_4^m, h_1^l, h_2^l\}$
Task dimension d	$25 \sim 50$
Number of source tasks K	\mathbb{N}^+
Source optimization algorithm \mathcal{A}	$\{\text{GA, PSO, CMAES, ...}\}$

- **Task family:** Eight single-objective functions with configurable optimal values serve as candidate families (see Supplementary Table B2). These functions are widely used in continuous optimization.
- **Transfer scenario:** Scenarios include intra-family transfer T_a , where source and target tasks belong to the same family, and inter-family transfer T_e , where they belong to different families.
- **Similarity distribution:** Three types of similarity distributions are examined: high, mixed, and low (see Supplementary Table B3).
- **Task dimension:** To avoid the curse of dimensionality, problem dimensions are set within a range of 25 to 50.
- **Number of source tasks:** This parameter is a positive integer, tailored to meet specific experimental needs.
- **Source optimization algorithm:** Any population-based optimizer, such as genetic algorithms (GA) [2], particle swarm optimization (PSO) [34], and covariance matrix adaptation evolution strategy (CMAES) [25], can be employed as the source optimization algorithm. Prior knowledge is generated by running these algorithms on source tasks.

Supplementary Table B4 provides the configurations for the 12 STOPS, divided into three categories based on similarity levels: high similarity (HS), mixed similarity (MS), and low similarity (LS).

- **HS:** The optimal solutions of source and target tasks are closely aligned in the common space, ensuring high transferability.
- **MS:** Four customized similarity distributions are employed to adjust the proportion of similarity values, providing a balanced challenge between HS and LS scenarios.
- **LS:** The optimal solutions of source and target tasks differ significantly, presenting the most challenging transfer conditions.

Each category includes four unique problems, spanning eight task families and two transfer scenarios, ensuring a diverse range of challenges for evaluation. The number of source tasks is set to 10. The source optimization algorithm is GA with a population size of 20 and a maximum of 250 iterations, yielding $10 \times 250 = 2500$ prior knowledge entries (populations and fitness data). For GA, we use simulated binary crossover [59], polynomial mutation [60], and 1/2 truncation selection, with parameters $p_c = 1$, $\eta_c = 15$, $p_m = 1/d$, and $\eta_m = 15$.

In Fig. 2b, we evaluate three source optimization algorithms: GA, PSO, and CMAES, each configured with a population size of 20 and a maximum of 250 iterations.

Table B2 Task family.

ID	Name	Formulation
f_1	Sphere	$\min f_1(\mathbf{x}) = \sum_{i=1}^d (x_i - o_i)^2, \mathbf{x} \in [-100, 100]$
f_2	Ellipsoid	$\min f_2(\mathbf{x}) = \sum_{i=1}^d (d - i + 1)(x_i - o_i)^2, \mathbf{x} \in [-50, 50]$
f_3	Schwefel 2,2	$\min f_3(\mathbf{x}) = \sum_{i=1}^d x_i - o_i + \prod_{i=1}^d x_i - o_i , \mathbf{x} \in [-30, 30]$
f_4	Quartic with noise	$\min f_4(\mathbf{x}) = \varepsilon + \sum_{i=1}^d i \times (x_i - o_i)^4, \mathbf{x} \in [-5, 5]$
f_5	Ackley	$\min f_5(\mathbf{x}) = -20 \exp \left(-0.2 \sqrt{\frac{1}{d} \sum_{i=1}^d x_i^2} \right) - \exp \left(\frac{1}{d} \sum_{i=1}^d \cos(2\pi z_i) \right) + 20 + e, z_i = x_i - o_i, \mathbf{x} \in [-32, 32]$
f_6	Rastrigin	$\min f_6(\mathbf{x}) = \sum_{i=1}^d [(x_i - o_i)^2 + 10 \cos(2\pi(x_i - o_i))] + 10d, \mathbf{x} \in [-10, 10]$
f_7	Griewank	$\min f_7(\mathbf{x}) = 1 + \frac{1}{4000} \sum_{i=1}^d (x_i - o_i)^2 - \prod_{i=1}^d \cos \left(\frac{x_i - o_i}{\sqrt{i}} \right), \mathbf{x} \in [-200, 200]$
f_8	Levy	$\min f_8(\mathbf{x}) = \sin^2(\pi \omega_1) + \sum_{i=2}^{d-1} (\omega_i - 1)^2 [1 + 10 \sin^2(\pi \omega_i + 1)] + (\omega_d - 1)^2 [1 + \sin^2(2\pi \omega_d)], \omega_i = 1 + \frac{z_i}{4}, \mathbf{x} \in [-20, 20]$

d is the problem dimension, x_i is the i -th decision variable, o_i represents the optimal solution of the i -th variable, and $\varepsilon \sim u(0, 1)$ denotes random noise.

Table B3 Similarity distribution.

Similarity	Distribution
High similarity	$h_1^h(s) = \delta(s-1) = \lim_{\sigma \rightarrow 0} \frac{1}{ \sigma \sqrt{\pi}} e^{-[(s-1)/\sigma]^2}$ $h_2^h(s) = \text{ReLU}(8s-4) = \frac{(8s-4) + 8s-4 }{2}$
Mixed similarity	$h_1^m(s) = 1$ $h_2^m(s) = 2s$ $h_3^m(s) = 2 - 2s$ $h_4^m(s) = \begin{cases} 4s, & 0 \leq s \leq 0.5 \\ 4 - 4s, & 0.5 \leq s \leq 1 \end{cases}$
Low similarity	$h_1^l(s) = \delta(s) = \lim_{\sigma \rightarrow 0} \frac{1}{ \sigma \sqrt{\pi}} e^{-(s/\sigma)^2}$ $h_2^l(s) = \text{ReLU}(4-8s) = \frac{(4-8s) + 4-8s }{2}$

Table B4 STOP benchmark suite.

Problem ID	Problem Configuration ($\gamma - T - h - d - K - \mathcal{A}$)	Similarity
STOP1	Sphere-Ta- h_1^h -50-10-GA	High Similarity
STOP2	Ellipsoid-Te- h_2^h -25-10-GA	
STOP3	Schwefel-Ta- h_2^h -30-10-GA	
STOP4	Quartic-Te- h_1^h -50-10-GA	
STOP5	Ackley-Ta- h_1^m -25-10-GA	Mixed Similarity
STOP6	Rastrigin-Te- h_2^m -50-10-GA	
STOP7	Griewank-Ta- h_3^m -25-10-GA	
STOP8	Levy-Te- h_4^m -30-10-GA	
STOP9	Sphere-Ta- h_1^l -25-10-GA	Low Similarity
STOP10	Rastrigin-Te- h_2^l -30-10-GA	
STOP11	Ackley-Ta- h_2^l -50-10-GA	
STOP12	Ellipsoid-Te- h_1^l -50-10-GA	

In Fig. 6a, the number of source tasks is varied to 10, 50, 100, and 1,000. For all configurations, GA serves as the source optimization algorithm, configured with a population size of 20 and a maximum of 250 iterations. This setup yields 2,500, 12,500, 25,000, and 250,000 prior knowledge entries, corresponding to 10, 50, 100, and 1,000 source tasks, respectively.

B.2 Baseline

The baseline encompasses four types of methods: no knowledge transfer (N), what to transfer, how to transfer, and when to transfer. The latter three categories specifically address how the knowledge carried by solutions from source tasks is transferred to the target task. Detailed implementations of these methods are provided in [21].

- **No knowledge transfer (N)** involves using evolutionary optimizers without incorporating any prior knowledge.

- **What to transfer** focuses on identifying solutions with the highest estimated transferability for target tasks. Evaluation metrics include:
 - Hamming distance (H)
 - Euclidean distance (M1)
 - Wasserstein distance (WD)
 - Ordinal correlation (OC)
 - Relaxed ordinal correlation (ROC)
 - Kullback-Leibler divergence (KLD)
- **How to transfer** aims at enhancing the quality of transferred solutions. These approaches typically involve adjusting solutions using the learned mapping between the source and target tasks. Techniques include:
 - Elite-based translation transformation (M1-Te)
 - Random individual-based translation transformation (M1-Tr)
 - Population mean-based translation transformation (M1-Tm)
 - Multiplication transformation using estimated means (M1-M)
 - Affine transformation (M2-A)
 - Linear transformation with ordinal correlation (OC-L)
 - Affine transformation with ordinal correlation (OC-A)
 - Kernel mapping (OC-K)
 - Neural network models (OC-N)
 - Latent-space connected linear transformations (ROC-L)
- **When to transfer** addresses timing decisions for knowledge transfer throughout the evolutionary process. This category includes fixed-interval methods, denoted as F1, F5, and F10, and adaptive methods such as:
 - Mixture model-based estimation (D-M)
 - Representation model-based estimation (D-G)
 - Population distribution-based estimation (D-P)

B.3 Parameter setting

All experiments are conducted on a Linux platform with a GPU 2080Ti (Memory: 12 GB, CUDA Version: 11.3). The parameter settings for all methods are provided as follows.

General settings:

- Number of independent runs: 20.
- Maximum number of evaluations F : 5000.

General settings for all baselines:

- Common search space: $[0, 1]^d$, where d represents the problem dimension.
- Backbone optimizer: A classical GA with simulated binary crossover [59], polynomial mutation [60], and 1/2 truncation selection, where p_c , η_c , p_m , and η_m are set to be 1, 15, $1/d$, and 15, respectively.
- Population size N : 20.

Parameter settings for what to transfer:

- Generation interval for transferring solutions G_t : 1.
- Number of source tasks k : 10.
- Number of candidate source tasks providing optimized solutions per transfer generation: 1.

Parameter settings for how to transfer:

- Generation interval for transferring solutions G_t : 1.
- Number of source tasks k : 10.
- Number of candidate source tasks providing optimized solutions per transfer generation: 1.
- Source selection: Permutations from 1 to k .

Parameter settings for when to transfer:

- Number of source tasks k : 10.
- Number of candidate source tasks providing optimized solutions per transfer generation: 1.
- Source selection: Permutations from 1 to k .

Parameter Settings for OKAEM:

- Architecture parameters:
 - Number of layers L : 1
 - Embedding dimension d_A : d
 - Number of attention heads H : 4
 - MLP hidden dimension d_M : 64
 - Dropout probability in crossover p_C : 0.95
 - Dropout probability in mutation p_M : 0.95
- Training parameters:
 - Learning rate lr : $1e - 3$
 - Weight decay wd : $1e - 2$
 - Batch size for pre-training: 256
- Evolutionary parameters:
 - Population size N : 20
 - Number of iterations T : 250

B.4 Supplementary experimental results

The ablation study of the crossover and mutation modules is shown in Table B5.

Table B5 Ablation study of crossover and mutation modules. The results, presented as objective values (average \pm standard deviations), are obtained over 20 independent runs. Symbols “+/ \approx /-” indicate that the baseline is significantly better/similar/worse than OKAEM on the Wilcoxon rank-sum test with a confidence level of 0.95, respectively.

Problem	OKAEM-Crossover Only	OKAEM-Mutation Only	OKAEM
STOP1	$1.47e + 03 \pm 9.79e + 05$	$2.61e + 03 \pm 2.49e + 06$	$1.30e + 00 \pm 1.44e + 00$
STOP2	$2.39e + 01 \pm 5.78e + 03$	$4.79e + 01 \pm 1.26e + 04$	$3.82e - 01 \pm 3.15e - 01$
STOP3	$1.18e + 01 \pm 8.79e + 01$	$2.56e + 01 \pm 2.60e + 02$	$7.47e - 01 \pm 2.98e + 00$
STOP4	$2.83e + 03 \pm 5.38e + 06$	$8.07e + 03 \pm 1.11e + 07$	$3.87e - 01 \pm 1.13e - 02$
STOP5	$1.49e + 01 \pm 3.41e + 00$	$7.10e + 00 \pm 1.21e + 01$	$2.46e - 02 \pm 2.31e - 04$
STOP6	$2.19e + 02 \pm 2.36e + 03$	$1.24e + 02 \pm 7.74e + 02$	$1.24e + 02 \pm 5.80e + 02$
STOP7	$9.07e - 01 \pm 2.82e - 01$	$7.19e - 02 \pm 1.07e - 02$	$7.75e - 03 \pm 7.33e - 05$
STOP8	$9.72e + 00 \pm 1.51e + 02$	$4.72e + 01 \pm 4.65e + 02$	$6.69e + 00 \pm 4.15e + 01$
STOP9	$1.69e - 02 \pm 4.67e - 04$	$4.14e + 02 \pm 5.70e + 05$	$2.34e - 03 \pm 4.59e - 06$
STOP10	$8.65e + 01 \pm 6.28e + 02$	$5.93e + 01 \pm 3.42e + 02$	$3.45e + 01 \pm 3.95e + 01$
STOP11	$2.79e + 00 \pm 3.26e + 01$	$1.81e + 01 \pm 7.32e - 01$	$2.53e + 00 \pm 1.61e + 01$
STOP12	$2.12e + 04 \pm 1.65e + 08$	$1.41e + 04 \pm 6.20e + 07$	$3.17e + 02 \pm 1.45e + 05$
+/ \approx /-	0/2/10	0/1/11	-

Appendix C Black-box optimization benchmark problem

C.1 Baseline

This paper aims to advance the development of population-based evolutionary computation. Therefore, we do not compare with non-population-based approaches such as Bayesian optimization, which struggles with continuous optimization problems exceeding 100 dimensions. Furthermore, we omit large language models-based approaches [61–63] from our baseline, as they are better suited for specific types of tasks. Our baseline includes classical EAs and their adaptive variants, as well as advanced learnable EAs.

Classical EAs and their adaptive variants:

- SimpleGA [37], one of the most popular EAs in black-box optimization.
- GA with group elite selection of mutation rates (GESMR-GA) [38], an advanced adaptive variant of GA.
- CMAES [25] and XNES [39], widely regarded as state-of-the-art EAs for addressing challenging continuous optimization problems (e.g., ill-conditioned, non-convex, non-continuous, or multi-modal).

Learnable EAs:

- Learnable GA (LGA) [26], which discovers new GAs in a data-driven manner, applicable to unseen optimization problems, search dimensions, and evaluation budgets.
- Learnable evolution strategy (LES) [27], which uses data-driven approaches to discover novel evolution strategies with strong generalization and search efficiency.

C.2 Parameter setting

All experiments are conducted on a Linux platform with a GPU 2080Ti (Memory: 12 GB, CUDA version: 11.3). The implementations of baselines are obtained from a JAX-based evolutionary strategies library [40]. For SimpleGA, GESMR-GA, CMAES, and XNES, the primary control parameters are automatically tuned. Other hyperparameters are optimized using grid search to identify the best combinations. For LGA and LES, we used the pre-trained parameters provided by the authors. All baselines are configured with a population size of 20 and a maximum of 200 generations. Detailed parameter settings are listed in Supplementary Table C6.

Table C6 Detailed parameter configurations for the baselines.

Algorithm	Parameter	Setting
SimpleGA	Initial $\sigma = 0.2$	We use grid search in $[0.1, 1]$ with a step size of 0.1.
	Crossover probability $p_c = 0.7$	We use grid search in $[0.5, 1]$ with a step size of 0.1.
GESMR-GA	Initial $\sigma = 0.2$	We use grid search in $[0.1, 1]$ with a step size of 0.1.
CMAES/XNES	Initial $\sigma = 0.2$	We use grid search in $[0.1, 1]$ with a step size of 0.1.
	Initial μ	$\mu = lb + \text{randn}(d) \times (ub - lb)$
LGA	All parameters	We use the pre-trained parameters provided by the authors.
LES	All parameters	We use the pre-trained parameters provided by the authors.

ub and lb are the upper and lower bounds of the problem, respectively. $\text{randn}(d)$ stands for sampling a d -dimensional vector from a standard normal distribution.

The parameter settings for OKAEM are provided as follows:

- Architecture parameters:
 - Number of layers L : 1
 - Embedding dimension d_A : 64
 - Number of attention heads H : 1
 - MLP hidden dimension d_M : 64
 - Dropout probability in crossover p_C : 0.95
 - Dropout probability in mutation p_M : 0.5
- Training parameters:
 - Learning rate lr : $1e - 3$
 - Weight decay wd : $1e - 5$

C.3 Supplementary experimental results

Performance comparison on 24 black-box optimization benchmark problems is shown in Fig. C1.

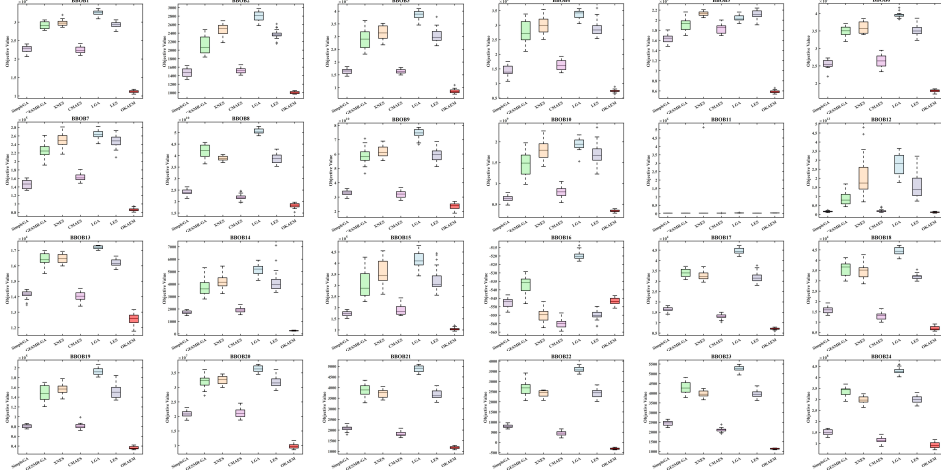


Fig. C1 Performance comparison on 24 black-box optimization benchmark problems (20 independent runs with random initialization, population size $N = 20$, number of iterations $T = 200$). The results are presented regarding objective values (lower is better).

Appendix D Prompt tuning for the vision-language model

D.1 Datasets

We conduct experiments on eight visual image classification datasets: Caltech101 [45], OxfordPets [46], StanfordCars [47], Food101 [48], UCF101 [49], SUN397 [50], EuroSAT [51], and DTD [52]. These datasets, covering a wide range of visual tasks, are commonly used to evaluate prompt tuning tasks. Their statistics are summarized in Supplementary Table D7.

- **Caltech101**, **OxfordPets**, and **StanfordCars** provide images for fine-grained classification and recognition. Caltech101 includes images of 101 object categories; OxfordPets features a diverse set of pet breeds; and StanfordCars offers detailed images of car models for precise vehicle identification.
- **Food101** focuses on food image classification, covering a broad spectrum of global cuisines.
- **UCF101** specializes in human action recognition from video clips, assessing both category-specific and dynamic scene understanding.
- **SUN397** provides a nearly exhaustive collection of scenes, suitable for evaluating scene recognition tasks.
- **EuroSAT** comprises satellite imagery for land use classification, representing various Earth surface covers from a spaceborne perspective.
- **DTD** targets the visual recognition of diverse textural patterns found in both natural and artificial surfaces.

D.2 Problem configuration

In alignment with the experimental setup in [64], the same 16-shot split for prompt tuning is employed across all methods. Evaluation is conducted on the full test sets for comparison.

Following the model configuration adopted in [41], the open-source CLIP model with ViT-B/32 is used as the backbone for the visual encoder. The intrinsic dimension is set to 1000. The vision prompt length and language prompt length are set to 8 and 5, respectively.

D.3 Parameter setting

All experiments are conducted on a Linux platform with a GPU 2080Ti (Memory: 12 GB, CUDA version: 11.3). The general settings are as follows:

- Loss function: Cross entropy.
- Number of independent runs: 5.
- Population size N : 12 for SUN397 to prevent memory overflow during parallel computing, and 20 for other datasets.
- Interval for calculating test accuracy: Every 12 evaluations.
- Maximum number of evaluations F : See Supplementary Table D7.

The configuration of the manual prompt is consistent with [53]. The main control parameters of CMAES are automatically adjusted. Other hyperparameters of CMAES are tuned using grid search to determine the optimal combination (see Supplementary Table C6 for specific settings). The parameter settings for OKAEM/OKAEM-FT are provided as follows:

- Prior Knowledge Generation: We perform prompt tuning on the Caltech101 dataset using CMAES with a population size of 20 and a maximum of 4800 evaluations. This setup generates a total of 240 prior knowledge entries (populations and fitness data).
- Architecture parameters:
 - Number of layers L : 1
 - Embedding dimension d_A : 512
 - Number of attention heads H : 1
 - MLP hidden dimension d_M : 64
 - Dropout probability in crossover p_C : 0.95
 - Dropout probability in mutation p_M : 0.5
- Training parameters:
 - Learning rate lr : $1e - 3$
 - Weight decay wd : $1e - 5$
 - Batch size for pre-training: 16

Table D7 Statistics of the datasets for prompt tuning in vision-language models.

Dataset	Classes	Train	Val	Test	Hand-crafted prompt	Maximum number of evaluations
Caltech101	100	4,128	1,649	2,465	"a photo of a [CLASS]."	4,800
OxfordPets	37	2,944	736	3,669	"a photo of a [CLASS], a type of pet."	4,800
StanfordCars	196	6,509	1,635	8,041	"a photo of a [CLASS]."	25,200
Food101	101	50,500	20,200	30,300	"a photo of [CLASS], a type of food."	4,800
UCF101	101	7,639	1,898	3,783	"a photo of a person doing [CLASS]."	25,200
SUN397	397	15,880	3,970	19,850	"a photo of a [CLASS]."	18,000
EuroSAT	10	13,500	5,400	8,100	"a centered satellite photo of [CLASS]."	25,200
DTD	47	2,820	1,128	1,692	"[[CLASS] texture."	36,000

References

- [1] Eiben, A.E., Smith, J.: From evolutionary computation to the evolution of things. *Nature* **521**(7553), 476–482 (2015)
- [2] Holland, J.H.: Outline for a logical theory of adaptive systems. *J. ACM* **9**(3), 297–314 (1962)
- [3] Ollivier, Y., Arnold, L., Auger, A., Hansen, N.: Information-geometric optimization algorithms: A unifying picture via invariance principles. *Journal of Machine Learning Research* **18**(18), 1–65 (2017)
- [4] Banzhaf, W., Nordin, P., Keller, R.E., Francone, F.D.: *Genetic Programming: an Introduction: on the Automatic Evolution of Computer Programs and Its Applications*. Morgan Kaufmann Publishers Inc., San Francisco, CA, USA (1998)
- [5] Miikkulainen, R., Forrest, S.: A biological perspective on evolutionary computation. *Nature Machine Intelligence* **3**(1), 9–15 (2021)
- [6] Stanley, K.O., Clune, J., Lehman, J., Miikkulainen, R.: Designing neural networks through neuroevolution. *Nature Machine Intelligence* **1**(1), 24–35 (2019)
- [7] Yan, M., Wang, R., Liu, K.: Populating cellular metamaterials on the extrema of attainable elasticity through neuroevolution. *arXiv preprint arXiv:2412.11112* (2024)
- [8] Heuthe, V.-L., Panizon, E., Gu, H., Bechinger, C.: Counterfactual rewards promote collective transport using individually controlled swarm microrobots. *Science Robotics* **9**(97), 5888 (2024)
- [9] Slade, P., Kochenderfer, M.J., Delp, S.L., Collins, S.H.: Personalizing exoskeleton assistance while walking in the real world. *Nature* **610**(7931), 277–282 (2022)
- [10] Li, B., Wei, Z., Wu, J., Yu, S., Zhang, T., Zhu, C., Zheng, D., Guo, W., Zhao, C., Zhang, J.: Machine learning-enabled globally guaranteed evolutionary computation. *Nature Machine Intelligence*, 1–11 (2023)
- [11] Romera-Paredes, B., Barekatin, M., Novikov, A., Balog, M., Kumar, M.P., Dupont, E., Ruiz, F.J., Ellenberg, J.S., Wang, P., Fawzi, O., et al.: Mathematical discoveries from program search with large language models. *Nature*, 1–3 (2023)
- [12] Zhang, S., Larsen, B., Sydnor, V.J., Zeng, T., An, L., Yan, X., Kong, R., Kong, X., Gur, R.C., Gur, R.E., Moore, T.M., Wolf, D.H., Holmes, A.J., Xie, Y., Zhou, J.H., Fortier, M.V., Tan, A.P., Gluckman, P., Chong, Y.S., Meaney, M.J., Deco, G., Satterthwaite, T.D., Yeo, B.T.T.: In vivo whole-cortex marker of excitation-inhibition ratio indexes cortical maturation and cognitive ability in youth. *Proceedings of the National Academy of Sciences* **121**(23), 2318641121

(2024)

- [13] De Jong, K.: Evolutionary computation: a unified approach. In: Proceedings of the Genetic and Evolutionary Computation Conference Companion. GECCO '17, pp. 373–388. Association for Computing Machinery, New York, NY, USA (2017)
- [14] Tan, K.C., Feng, L., Jiang, M.: Evolutionary transfer optimization - a new frontier in evolutionary computation research. *IEEE Computational Intelligence Magazine* **16**(1), 22–33 (2021)
- [15] Scott, E.O., De Jong, K.A.: First complexity results for evolutionary knowledge transfer. In: Proceedings of the 17th ACM/SIGEVO Conference on Foundations of Genetic Algorithms. FOGA '23, pp. 140–151. Association for Computing Machinery, New York, NY, USA (2023)
- [16] Louis, S.J., McDonnell, J.: Learning with case-injected genetic algorithms. *IEEE Transactions on Evolutionary Computation* **8**(4), 316–328 (2004)
- [17] Huang, C., Li, Y., Yao, X.: A survey of automatic parameter tuning methods for metaheuristics. *IEEE Transactions on Evolutionary Computation* **24**(2), 201–216 (2020)
- [18] Nomura, M., Watanabe, S., Akimoto, Y., Ozaki, Y., Onishi, M.: Warm starting cma-es for hyperparameter optimization. *Proceedings of the AAAI Conference on Artificial Intelligence* **35**(10), 9188–9196 (2021)
- [19] Wang, C., Zhao, J., Li, L., Jiao, L., Liu, F., Liu, X., Yang, S.: Knowledge-aware evolutionary graph neural architecture search. *Knowledge-Based Systems* **309**, 112810 (2025)
- [20] Wang, C., Liu, J., Wu, K., Wu, Z.: Solving multitask optimization problems with adaptive knowledge transfer via anomaly detection. *IEEE Transactions on Evolutionary Computation* **26**(2), 304–318 (2022)
- [21] Xue, X., Yang, C., Feng, L., Zhang, K., Song, L., Tan, K.C.: Solution transfer in evolutionary optimization: An empirical study on sequential transfer. *IEEE Transactions on Evolutionary Computation* **28**(6), 1776–1793 (2024)
- [22] Turing, A.M.: In: Epstein, R., Roberts, G., Beber, G. (eds.) *Computing Machinery and Intelligence*, pp. 23–65. Springer, Dordrecht (2009)
- [23] Bäck, T., *et al.*: Self-adaptation in genetic algorithms. In: Proceedings of the First European Conference on Artificial Life, pp. 263–271 (1992). MIT press Cambridge
- [24] Schwefel, H.-P.: Evolution strategies: A family of non-linear optimization techniques based on imitating some principles of organic evolution. *Annals of*

- [25] Hansen, N.: The cma evolution strategy: A tutorial. arXiv preprint arXiv:1604.00772 (2016)
- [26] Lange, R.T., Schaul, T., Chen, Y., Lu, C., Zahavy, T., Dalibard, V., Flennerhag, S.: Discovering attention-based genetic algorithms via meta-black-box optimization. In: Proceedings of the Genetic and Evolutionary Computation Conference. GECCO '23, pp. 929–937. Association for Computing Machinery, New York, NY, USA (2023)
- [27] Lange, R.T., Schaul, T., Chen, Y., Zahavy, T., Dalibard, V., Lu, C., Singh, S., Flennerhag, S.: Discovering evolution strategies via meta-black-box optimization. In: The Eleventh International Conference on Learning Representations (2023)
- [28] Cao, Y., Chen, T., Wang, Z., Shen, Y.: Learning to optimize in swarms. In: Wallach, H., Larochelle, H., Beygelzimer, A., Alché-Buc, F., Fox, E., Garnett, R. (eds.) Advances in Neural Information Processing Systems, vol. 32 (2019)
- [29] Hong, H., Jiang, M.: Pre-evolved model for complex multi-objective optimization problems. arXiv preprint arXiv:2312.06125 (2023)
- [30] Li, X., Wu, K., Zhang, X., Wang, H., Liu, J.: B2opt: Learning to optimize black-box optimization with little budget. arXiv preprint arXiv:2304.11787 (2023)
- [31] Vaswani, A., Shazeer, N., Parmar, N., Uszkoreit, J., Jones, L., Gomez, A.N., Kaiser, L.u., Polosukhin, I.: Attention is all you need. In: Guyon, I., Luxburg, U.V., Bengio, S., Wallach, H., Fergus, R., Vishwanathan, S., Garnett, R. (eds.) Advances in Neural Information Processing Systems, vol. 30 (2017)
- [32] Loshchilov, I., Hutter, F.: Decoupled weight decay regularization. In: International Conference on Learning Representations (2019)
- [33] Xue, X., Yang, C., Feng, L., Zhang, K., Song, L., Tan, K.C.: A scalable test problem generator for sequential transfer optimization. arXiv preprint arXiv:2304.08503 (2023)
- [34] Kennedy, J., Eberhart, R.: Particle swarm optimization. In: Proceedings of ICNN'95 - International Conference on Neural Networks, vol. 4, pp. 1942–19484 (1995)
- [35] Hansen, N., Auger, A., Ros, R., Mersmann, O., Tušar, T., Brockhoff, D.: Coco: a platform for comparing continuous optimizers in a black-box setting. Optimization Methods and Software **36**(1), 114–144 (2021)
- [36] Hansen, N., Auger, A., Ros, R., Finck, S., Pošík, P.: Comparing results of 31 algorithms from the black-box optimization benchmarking bbob-2009. In: Proceedings

of the 12th Annual Conference Companion on Genetic and Evolutionary Computation. GECCO '10, pp. 1689–1696. Association for Computing Machinery, New York, NY, USA (2010)

- [37] Such, F.P., Madhavan, V., Conti, E., Lehman, J., Stanley, K.O., Clune, J.: Deep neuroevolution: Genetic algorithms are a competitive alternative for training deep neural networks for reinforcement learning. arXiv preprint arXiv:1712.06567 (2017)
- [38] Kumar, A., Liu, B., Miikkulainen, R., Stone, P.: Effective mutation rate adaptation through group elite selection. In: Proceedings of the Genetic and Evolutionary Computation Conference. GECCO '22, pp. 721–729. Association for Computing Machinery, New York, NY, USA (2022)
- [39] Wierstra, D., Schaul, T., Glasmachers, T., Sun, Y., Peters, J., Schmidhuber, J.: Natural evolution strategies. *J. Mach. Learn. Res.* **15**(1), 949–980 (2014)
- [40] Lange, R.T.: evosax: Jax-based evolution strategies. In: Proceedings of the Companion Conference on Genetic and Evolutionary Computation. GECCO '23 Companion, pp. 659–662. Association for Computing Machinery, New York, NY, USA (2023)
- [41] Yu, L., Chen, Q., Lin, J., He, L.: Black-box prompt tuning for vision-language model as a service. In: Elkind, E. (ed.) Proceedings of the Thirty-Second International Joint Conference on Artificial Intelligence, IJCAI-23, pp. 1686–1694 (2023). Main Track
- [42] Sun, T., Shao, Y., Qian, H., Huang, X., Qiu, X.: Black-box tuning for language-model-as-a-service. In: Chaudhuri, K., Jegelka, S., Song, L., Szepesvari, C., Niu, G., Sabato, S. (eds.) Proceedings of the 39th International Conference on Machine Learning. Proceedings of Machine Learning Research, vol. 162, pp. 20841–20855 (2022)
- [43] Sun, T., He, Z., Qian, H., Zhou, Y., Huang, X., Qiu, X.: BBTv2: Towards a gradient-free future with large language models. In: Goldberg, Y., Kozareva, Z., Zhang, Y. (eds.) Proceedings of the 2022 Conference on Empirical Methods in Natural Language Processing, pp. 3916–3930. Association for Computational Linguistics, Abu Dhabi, United Arab Emirates (2022)
- [44] Wang, C., Zhao, J., Jiao, L., Li, L., Liu, F., Yang, S.: When large language models meet evolutionary algorithms. arXiv preprint arXiv:2401.10510 (2024)
- [45] Fei-Fei, L., Fergus, R., Perona, P.: Learning generative visual models from few training examples: An incremental bayesian approach tested on 101 object categories. In: 2004 Conference on Computer Vision and Pattern Recognition Workshop, pp. 178–178 (2004). IEEE

- [46] Parkhi, O.M., Vedaldi, A., Zisserman, A., Jawahar, C.: Cats and dogs. In: 2012 IEEE Conference on Computer Vision and Pattern Recognition, pp. 3498–3505 (2012). IEEE
- [47] Krause, J., Stark, M., Deng, J., Fei-Fei, L.: 3d object representations for fine-grained categorization. In: Proceedings of the IEEE International Conference on Computer Vision (ICCV) Workshops (2013)
- [48] Bossard, L., Guillaumin, M., Van Gool, L.: Food-101 – mining discriminative components with random forests. In: Fleet, D., Pajdla, T., Schiele, B., Tuytelaars, T. (eds.) Computer Vision – ECCV 2014, pp. 446–461. Springer, Cham (2014)
- [49] Soomro, K.: Ucf101: A dataset of 101 human actions classes from videos in the wild. arXiv preprint arXiv:1212.0402 (2012)
- [50] Xiao, J., Hays, J., Ehinger, K.A., Oliva, A., Torralba, A.: Sun database: Large-scale scene recognition from abbey to zoo. In: 2010 IEEE Computer Society Conference on Computer Vision and Pattern Recognition, pp. 3485–3492 (2010)
- [51] Helber, P., Bischke, B., Dengel, A., Borth, D.: Eurosat: A novel dataset and deep learning benchmark for land use and land cover classification. *IEEE Journal of Selected Topics in Applied Earth Observations and Remote Sensing* **12**(7), 2217–2226 (2019)
- [52] Cimpoi, M., Maji, S., Kokkinos, I., Mohamed, S., Vedaldi, A.: Describing textures in the wild. In: 2014 IEEE Conference on Computer Vision and Pattern Recognition, pp. 3606–3613 (2014)
- [53] Radford, A., Kim, J.W., Hallacy, C., Ramesh, A., Goh, G., Agarwal, S., Sastry, G., Askell, A., Mishkin, P., Clark, J., Krueger, G., Sutskever, I.: Learning transferable visual models from natural language supervision. In: Meila, M., Zhang, T. (eds.) Proceedings of the 38th International Conference on Machine Learning. Proceedings of Machine Learning Research, vol. 139, pp. 8748–8763 (2021)
- [54] Qian, H., Hu, Y.-Q., Yu, Y.: Derivative-free optimization of high-dimensional non-convex functions by sequential random embeddings. In: Proceedings of the Twenty-Fifth International Joint Conference on Artificial Intelligence. IJCAI’16, pp. 1946–1952 (2016)
- [55] Tian, Y., Si, L., Zhang, X., Cheng, R., He, C., Tan, K.C., Jin, Y.: Evolutionary large-scale multi-objective optimization: A survey. *ACM Comput. Surv.* **54**(8) (2021)
- [56] Deb, K., Pratap, A., Agarwal, S., Meyarivan, T.: A fast and elitist multiobjective genetic algorithm: Nsga-ii. *IEEE Transactions on Evolutionary Computation* **6**(2), 182–197 (2002)

- [57] Zhang, Q., Li, H.: Moea/d: A multiobjective evolutionary algorithm based on decomposition. *IEEE Transactions on Evolutionary Computation* **11**(6), 712–731 (2007)
- [58] Su, J., Ahmed, M., Lu, Y., Pan, S., Bo, W., Liu, Y.: Roformer: Enhanced transformer with rotary position embedding. *Neurocomputing* **568**, 127063 (2024)
- [59] Deb, K., Agrawal, R.B., *et al.*: Simulated binary crossover for continuous search space. *Complex systems* **9**(2), 115–148 (1995)
- [60] Deb, K., Goyal, M., *et al.*: A combined genetic adaptive search (geneas) for engineering design. *Computer Science and informatics* **26**, 30–45 (1996)
- [61] Meyerson, E., Nelson, M.J., Bradley, H., Gaier, A., Moradi, A., Hoover, A.K., Lehman, J.: Language model crossover: Variation through few-shot prompting. *ACM Trans. Evol. Learn. Optim.* **4**(4) (2024)
- [62] Lehman, J., Gordon, J., Jain, S., Ndousse, K., Yeh, C., Stanley, K.O.: In: Banzhaf, W., Machado, P., Zhang, M. (eds.) *Evolution Through Large Models*, pp. 331–366. Springer, Singapore (2024)
- [63] Yang, C., Wang, X., Lu, Y., Liu, H., Le, Q.V., Zhou, D., Chen, X.: Large language models as optimizers. In: *The Twelfth International Conference on Learning Representations* (2024)
- [64] Zhou, K., Yang, J., Loy, C.C., Liu, Z.: Learning to prompt for vision-language models. *International Journal of Computer Vision* **130**(9), 2337–2348 (2022)